

Synthesis and Characterization of Aluminated Santa Barbara Amorphous-15 via Ultrasonic-Enhanced Hydrothermal Method: Effects of Sonication, Solvent Acidity, and Si/Al Ratio

Dini Hariyanto Putri ¹, R. R. Dirgarini Julia Nurlianti Subagyo ^{1,*},
 Veliyana Londong Allo ¹, Maykel Manawan ^{2,3}

¹ Physical Chemistry Laboratory, Faculty of Mathematics and Natural Sciences, Mulawarman University, Samarinda 75124, Indonesia

² Faculty of Defense Science and Technology, Universitas Pertahanan - RI, Bogor 16810, Indonesia

³ Research Center of Advanced Materials, National Research and Innovation Agency, Serpong 15314, Indonesia

* Corresponding author: dirgarini@fmipa.unmul.ac.id

<https://doi.org/10.14710/jksa.28.6.292-298>

Article Info

Article history:

Received: 27th April 2025

Revised: 04th July 2025

Accepted: 08th July 2025

Online: 05th August 2025

Keywords:

Synthesis; Al-SBA-15;
 Ultrasonication; Hydrothermal
 Method

Abstract

Aluminated Santa Barbara Amorphous-15 (Al-SBA-15) materials were successfully synthesized using an ultrasonic-enhanced hydrothermal method. The synthesis was conducted by varying the mole ratio of Si precursor and Al precursor (10 and 20), sonication time (3 and 5 hours), and solvent type (2 M hydrochloric acid (HCl) and distilled water). The resulting materials were characterized using N₂ sorption analyzer, Fourier Transform Infrared Spectroscopy (FTIR), Small-Angle X-ray Diffraction (SAXRD), Scanning Electron Microscopy (SEM), and Ammonia-Temperature Programmed Desorption (NH₃-TPD). FTIR spectra confirmed the presence of siloxane, silanol, and hydroxyl functional groups in all Al-SBA-15 samples. SAXRD analysis showed three characteristic peaks of SBA-15, indicating a two-dimensional hexagonal structure (p6mm). Increasing the sonication time enhanced the surface area from 718 to 767 m²/g, while reducing the pore diameter from 5.96 to 4.81 nm and the pore volume from 1.07 to 0.92 cm³/g. Raising the Si:Al molar ratio slightly increased the surface area (718 to 722 m²/g) and decreased the pore diameter and volume. Additionally, using distilled water instead of 2 M HCl as the solvent raised the surface area from 722 to 785 m²/g, while decreasing the pore diameter from 5.61 to 5.05 nm and slightly lowering the pore volume. The acidity of the Al-SBA-15 material varied according to the sonication time and the amount of Al precursor used, suggesting the potential of regulating the acidic properties through optimization of the synthesis parameters.

1. Introduction

The synthesis of materials for various applications continues to expand through the development of diverse methods. Despite providing significant benefits, well-established methods often generate hazardous chemical waste that negatively impacts the environment. With the increasing awareness of sustainability, the concept of green chemistry is being applied to develop cleaner, more efficient, and environmentally friendly synthesis processes, with a focus on reducing hazardous waste and improving the safety of the synthesis process [1].

One of the most widely developed materials is a catalyst with a large surface area and physicochemical properties that can be controlled. Mesoporous silica, such as Santa Barbara Amorphous-15 (SBA-15), effectively supports catalysts due to its high surface area. This material can be synthesized using various methods, most of which employ specific templates to control the pore structure, such as the microemulsion template method [2], the ionic block copolymer template method [3], the emulsion-mediated method using oil [4], or the hydrothermal method using structure-directing molecules [5].

SBA-15 is a mesoporous material characterized by an organised hexagonal architecture, exhibiting elevated surface areas, significant pore volumes [6]. In addition to its mesopores, SBA-15 contains micropores within its pore walls, which enhance its surface area and pore volume and are advantageous for adsorption and catalysis [7]. The properties of SBA-15 enable this mesoporous material to be suitable for use as a catalyst support [8, 9] and adsorbent [10, 11]. SBA-15 exhibits greater hydrothermal stability than Mobil Composition of Matter No. 41 (MCM-41) and Hexagonal Mesoporous Silica (HMS), which possess a hexagonal structure, owing to their thicker pore walls [12]. However, pure silica-based SBA-15 has a limited number of acid sites, which can be a drawback in certain catalytic applications.

Increased acidity can be achieved by metal doping into the SBA-15 framework [13]; one of which uses aluminium to produce Al-SBA-15. This modification aims to introduce more Brønsted acid sites into the structure, improving catalytic performance. The addition of other metals, such as nickel, is also reported to enrich Lewis acid sites and improve the catalytic properties of SBA-15 [14]. Thus, the addition of aluminium is based on its ability to enhance both the structural stability and acidity of the SBA-15 framework. Incorporating Al into the silica network in place of silicon has been shown to increase the number of acid sites and improve catalytic performance [14].

The choice of synthesis method is crucial to produce Al-SBA-15 with optimal characteristics. The hydrothermal method, involving the formation of sol and gel, is a common approach involving the formation of a homogeneous precursor solution at the molecular level, followed by polymerization into a gel [15]. The hydrothermal method, which involves the formation of sol and gel, is a widely used technique wherein a homogeneous precursor solution is prepared at the molecular level and subsequently polymerized into a gel [15]. However, this process is relatively slow (up to 24 hours in the hydrolysis process) and sometimes results in a less uniform particle size distribution [5, 15]. One approach to overcoming these limitations is using ultrasonic irradiation (sonication) to accelerate sol–gel reactions. Sonication produces strong mechanical vibrations that accelerate chemical reactions and improve material homogeneity [16]. The combination of the hydrothermal method and sonication offers great potential in improving the structure and properties of the synthesized material [14].

This study aims to prepare Al-SBA-15 material using the ultrasonic-enhanced hydrothermal method. The novelty in this study is the use of sonication to accelerate the synthesis while evaluating the effect of variation in sonication time, solvent acidity, and mole ratio of Si precursor and Al precursor on the characteristics of the resulting mesoporous material. Previous studies have demonstrated that ultrasonic treatment improves precursor dispersion and facilitates the formation of a more uniform mesostructure, resulting in materials with increased surface areas and enhanced porosity [17, 18]. The acidity of the solvent was evaluated as it may affect

the hydrolysis–condensation kinetics and the template–silica interaction, while the Si:Al ratio may influence the material's acidity and catalytic performance. The resulting materials synthesized under different conditions were characterized with a BET surface area and pore size analyzer, Fourier transform infrared (FTIR), small-angle X-ray diffraction (SAXRD), scanning electron microscopy (SEM), and ammonia temperature programmed desorption (NH₃-TPD).

2. Experimental

2.1. Equipment

The equipment used were an analytical balance (Precision Instruments), oven (Kirin KBO-90M), desiccator, set of glassware, thermometer, pH meter (Hanna Instruments HI98107), porcelain cup, Krisbow Vacuum Pump 3/4 HP ERSV07, Buchner funnel, furnace (Kalstein Model YR 05273), and Krisbow Ultrasonic Cleaner 1400 mL with Ultrasonic Frequency 42 kHz.

2.2. Chemicals

The chemicals used were Pluronic 123 (poly(ethylene glycol)-block-poly(propylene glycol) block-poly(propylene glycol)) (Sigma-Aldrich), 32% hydrochloric acid (Allinckrodt), tetraethylorthosilicate (TEOS) (Sigma-Aldrich), aluminum nitrate nonahydrate (Al(NO₃)₃·9H₂O) (Merck KGaA), and Whatman 42 filter paper.

2.3. Al-SBA-15 Synthesis

The synthesis of Al-SBA-15 mesoporous silica material was carried out using a modification of the method of Zhao *et al.* [15] and Sarah *et al.* [16]. Sixteen grams of Pluronic 123 were added to an Erlenmeyer flask containing 640 mL of 2 M HCl solution and dissolved by stirring at room temperature until complete dissolution occurred (Solution A). Solution B was prepared by dissolving 3.46 g of Al(NO₃)₃·9H₂O in distilled water (mole ratio of Si to Al precursors = 20) or 6.91 g of Al(NO₃)₃·9H₂O in distilled water (mole ratio of Si to Al precursors = 10). Solution A was subjected to sonication at an ultrasonic frequency of 42 kHz for 10 minutes, after which solution B was incorporated into solution A. After 30 minutes of mixing, 38.4 mL of TEOS was added dropwise, and the mixture was subjected to sonication for a duration of either 3 or 5 hours at 40–50°C, depending on the targeted sample code (e.g., 103A for 3 hours sonication, 105A for 5 hours sonication, Table 1).

Table 1. The synthesis conditions of Al-SBA-15

Sample code	Molar ratio of Si and Al precursors	Solvent	Sonication time (hour)
Al-SBA-15 203A	20	HCl 2 M	3
Al-SBA-15 103A	10	HCl 2 M	3
Al-SBA-15 105A	10	HCl 2 M	5
Al-SBA-15 203	20	Distilled water	3

The mixture was then subjected to an oven at 100°C for 24 hours to undergo the hydrothermal aging process. The mixture was allowed to cool to room temperature and then filtered with a Buchner funnel and vacuum pump until a white solid was obtained. During the filtration procedure, the white particles were rinsed with distilled water until the pH of the filtrate matched that of distilled water. The resultant white solid was dried in an oven at 100°C and subsequently calcined at 500°C for 16 hours. The outcome achieved was a white, fine powder. In order to investigate the effect of solvent acidity, a comparative synthesis was conducted using 640 mL of distilled water to dissolve Pluronic 123 instead of 2 M HCl, while all other synthesis conditions were kept constant. In addition, after the sonication process for 3 hours, the mixture was allowed to stand for 48 hours at room temperature before aging. The variation of synthesis conditions and the naming of the resulting materials are shown in Table 1.

Characterization of Al-SBA-15 material was carried out using several instruments. Surface area, pore diameter, and pore volume were analyzed with the BET surface area and pore size analyzer Nova Touch LX-4 with a degassing temperature of 150°C. FTIR Bruker Alpha II was used to determine the functional groups of the material produced. Small-angle XRD analysis was conducted using a D-8 Advance XRD instrument under the following conditions: 20 kV/5 mA, divergence slit 0.1, Soller slit 2.5°, and LYNXEYE-XET detector with a 5.8° opening. The acidity of the catalyst was determined by NH₃-TPD analysis using a ChemiSorb 2750 instrument (Micromeritics). Surface morphology was observed using a Phenom X5 Pro Desktop SEM (Thermo Fisher Scientific).

3. Results and Discussion

SAXRD analysis of the synthesized Al-SBA-15 materials (Figure 1) shows three clear diffraction peaks, attributed to the (100), (110), and (200) planes, respectively. These three planes are characteristic of a two-dimensional hexagonal mesoporous structure with p6mm symmetry [15, 19], which confirms that the Al-SBA-15 material has been successfully synthesized with high mesostructure regularity.

Peak (100) has a dominant intensity, while peaks (110) and (200) appear with weak intensity at larger 2θ angles, following the typical diffraction pattern of SBA-15 [15]. A shift of the diffraction peaks towards larger angles was observed as the sonication time increased. This shift indicates a decrease in the lattice spacing (d_{100}), indicating a contraction in the mesoporous framework [16].

In addition, increasing the molar ratio of Si and Al precursors and the use of acid solvents also caused the (100), (110), and (200) diffraction peaks to shift more to the right. This indicates that modification of Si and Al composition and synthesis conditions affects the regularity and shrinkage of the mesoporous structure formed. Presumably, the integration of Al into the silica framework through condensation reactions results in a denser structure [20].

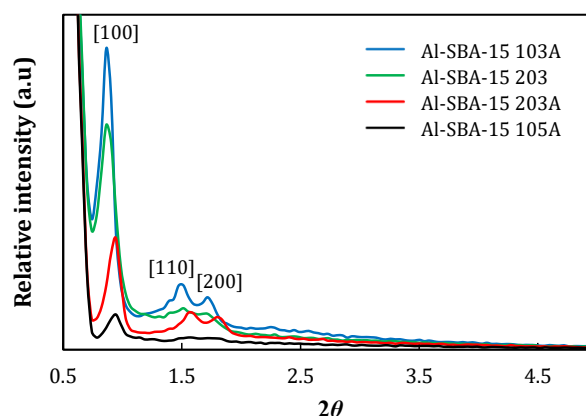


Figure 1. SAXRD patterns of Al-SBA-15 materials

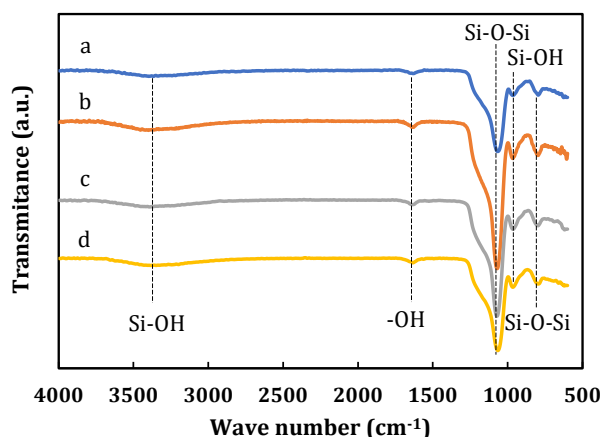


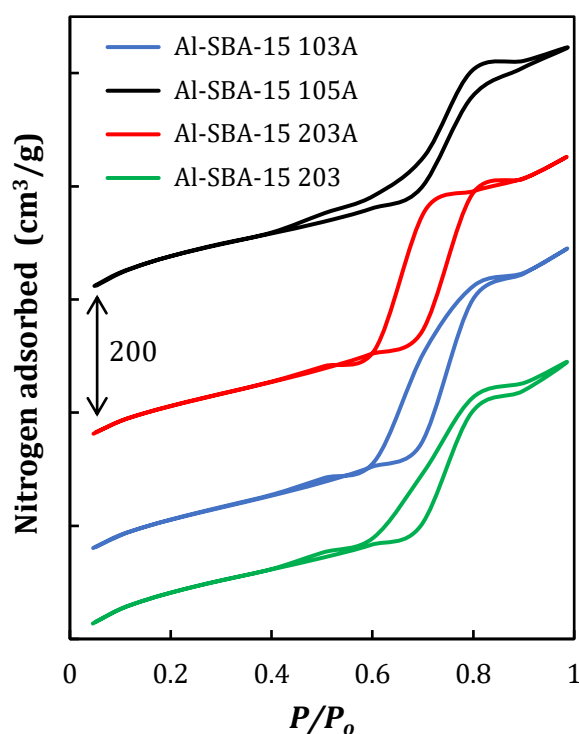
Figure 2. The FTIR spectra of Al-SBA-15 materials: (a) Al-SBA-15 105A, (b) Al-SBA-15 103A, (c) Al-SBA-15 203A, (d) Al-SBA-15 203

FTIR analysis was conducted to identify functional groups in the Al-SBA-15 materials and compared with those of SBA-15 to examine the effect of aluminum incorporation into the silica framework. The FTIR spectra of Al-SBA-15 material (Figure 2) show absorption bands at 3100–3700 cm⁻¹, indicating the excitation of H-bonded groups from Si-OH [21]. More specifically, in the Al-SBA-15 203A material, there is an absorption at 3418 cm⁻¹ associated with silanol hydroxyl groups and adsorbed water molecules, as well as an absorption at 1620 cm⁻¹ indicating adsorbed water vibrations. Anti-symmetric and symmetric stretching siloxane groups are characterized by absorption at 1050 cm⁻¹ and 776 cm⁻¹, while symmetric stretching silanol groups are seen at 960 cm⁻¹ [16]. Al-SBA-15 103A, Al-SBA-15 105A, and Al-SBA-15 203 materials show similar patterns with absorption bands at slightly different wavelengths (Table 2).

When compared to a study by Xie and Hu [22] on pure SBA-15 material, the absorption bands of the synthesized Al-SBA-15 material have slightly shifted, especially for the Si-O-Si (anti-symmetric stretching) (Table 2). This shift indicates that the integration of aluminium metal into the SBA-15 framework affects the chemical environment of the molecule and strengthens the Al-O bond compared to the Si-O [21]. This may be due to the smaller ionic radius of Al and its lower electronegativity than Si, resulting in stronger metal-oxide interactions [23].

Table 2. Comparison of FTIR absorption bands of Al-SBA-15 materials

Functional group	Wave number (cm ⁻¹)				
	Al-SBA-15 203A	Al-SBA-15 103A	Al-SBA-15 105A	Al-SBA-15 203	SBA-15* [22]
Si-O-Si (symmetric stretching)	776	796	795	790	780
Si-OH (symmetric stretching)	960	965	966	965	950
Si-O-Si (anti-symmetric stretching)	1050	1069	1066	1065	1080
-OH (bending vibration)	1620	1629	1631	-	1635
-OH (silanol)	3418	3408	3366	3349	3460

**Figure 3.** N₂ adsorption-desorption isotherm curves of Al-SBA-15 materials

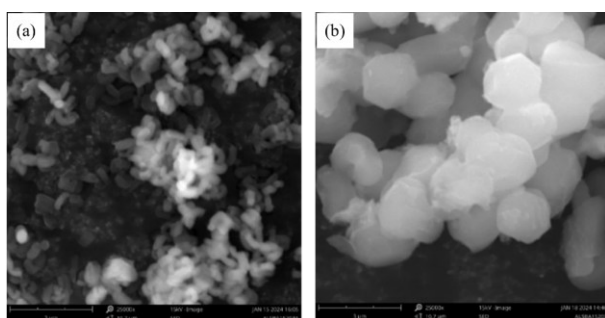
The N₂ adsorption/desorption isotherm curves of all Al-SBA-15 materials synthesized in this study show a type IV isotherm curve with H1 type hysteresis loop [15] (Figure 3). Thus, these isotherms confirm that all the synthesized Al-SBA-15 materials are mesoporous. The appearance of the hysteresis loop is due to capillary condensation, which occurs because the pore width exceeds a certain size, depending on the adsorption system and temperature [24]. The isotherm curve also shows the difference in the amount of nitrogen gas in the adsorption and desorption process. At the same relative pressure, a larger amount of nitrogen remains on the material surface during desorption than during adsorption, resulting in a hysteresis loop. At a relative pressure (P/P_0) of ≤ 0.6 , nitrogen gas adsorption forms a monolayer; as the relative pressure increases to ≥ 0.6 , multilayer adsorption occurs. Based on the isotherm, the total nitrogen adsorbed of the synthesized Al-SBA-15 materials ranges from 600 to 700 cm³/g, with the highest uptake observed in sample Al-SBA-15 203.

Increasing the concentration of the aluminium precursor (i.e., reducing the Si/Al molar ratio) results in a slight decrease in surface area, with an increase in pore diameter and pore volume, as shown in the samples Al-SBA-15 203A (Si/Al = 20) and Al-SBA-15 103A (Si/Al = 10) (Table 3). The surface area showed a minimal change from 722 m²/g to 718 m²/g, which is within the expected range of variation for BET measurements. Meanwhile, the pore diameter increased from 5.61 nm to 5.96 nm, and the pore volume rose from 1.01 to 1.07 cm³/g. The effect of Al incorporation was studied by comparing these values with those of an SBA-15 sample synthesized without aluminum under similar synthesis conditions [9], which had a surface area of 652 m²/g, a pore diameter of 7.72 nm, and a pore volume of 1.31 cm³/g. These results suggest that aluminium incorporation may affect pore size development, resulting in narrower mesopores and slightly lower pore volumes, while enhancing the surface area under optimized conditions. The observed changes align with previous findings, indicating that incorporation of aluminium can affect the mesostructure by distorting the silica network, decreasing wall regularity, and influencing pore dimensions [15, 25].

In addition, variations in sonication time showed that longer sonication increased the surface area of the materials but decreased their pore diameter and volume. For example, Al-SBA-15 105A (5 hours of sonication) exhibited a higher surface area (767 m²/g) than Al-SBA-15 103A (3 hours of sonication), which had a surface area of 716 m²/g. However, the pore diameter and volume of Al-SBA-15 103A were larger (5.96 nm and 1.07 cm³/g, respectively) than those of Al-SBA-15 105A, which were 4.81 nm and 0.92 cm³/g. The results can be attributed to the sonication mechanism, in which ultrasonic waves induce acoustic cavitation (the formation and collapse of microbubbles within the solution). This cavitation improves the mixing and dispersion of precursors on the molecular scale [26]. Sonication for a sufficiently long time (e.g., 3 hours) helps a more homogeneous distribution between Pluronic 123 surfactant as template and TEOS as silica source, thus forming denser pore walls and higher surface area [27]. However, excessive sonication (e.g., 5 hours) potentially destabilizes the mesoporous structure, causing the pore walls to become thinner or partially collapse, resulting in decreased pore diameter and volume [28].

Table 3. Surface area, pore diameter, and pore volume of Al-SBA-15 synthesized under various conditions

Material	Surface area (m ² /g)	Pore diameter (nm)	Pore volume (cm ³ /g)
Al-SBA-15 203A	722	5.61	1.01
Al-SBA-15 103A	718	5.96	1.07
Al-SBA-15 105A	767	4.81	0.92
Al-SBA-15 203	785	5.05	0.99
Al-SBA-15 (stirring for 20 hours, Si/Al=20) [19]	448	11.3	1.45

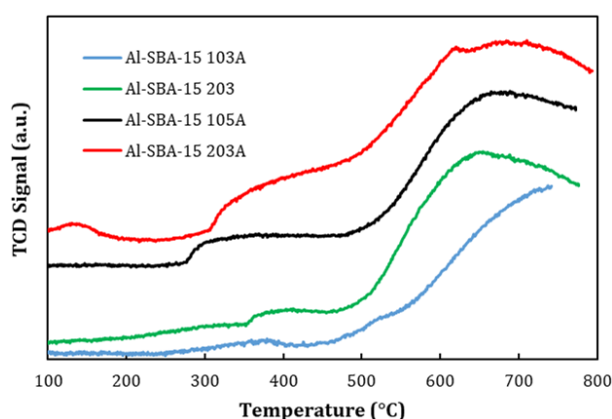
**Figure 4.** SEM images of Al-SBA-15 (a) 203A and (b) 203 with 25,000× magnification

Compared to the Al-SBA-15 material synthesized under similar conditions using Pluronic 123 as a template and TEOS as the silica source, but with 20 hours of conventional stirring (non-sonication) [19], the sonication-assisted material synthesized in this study exhibits a higher surface area (722–785 m²/g vs. 448 m²/g) (Table 3). This indicates that the sonication method significantly improves the dispersion of the precursors and forms a more ordered silica network structure in a shorter time. Meanwhile, the pore diameter and pore volume of the samples with sonication were lower than those of the non-sonicated samples. This is possible because the use of ultrasonic waves accelerates the formation of silica walls around the surfactant template, resulting in smaller pore sizes [17].

The use of acidic solvents (2 M HCl) compared to distilled water resulted in a decrease in surface area (from 785 to 722 m²/g), alongside a slight increase in pore diameter (from 5.05 to 5.61 nm) and pore volume (from 0.99 to 1.01 cm³/g) (Table 3). Under acidic conditions, the hydrolysis of TEOS was facilitated by the protonation of ethoxy groups, resulting in the formation of silanol (Si–OH). The following condensation could occur rapidly because of the high proton concentration; however, the fast polycondensation rate may disrupt the self-assembly involving the Pluronic 123 template. Wang *et al.* [29] found an increase in the rate of silica polycondensation in acidic conditions, which can result in larger pores but with less uniform pore size distribution and lower surface areas. In contrast, water, acting as a neutral solvent, may slow these processes, facilitating improved template–silica interaction and yielding an increased surface area.

Table 4. The acidity of Al-SBA-15 materials

No.	Material	Acidity (mmol/g)
1	Al-SBA-15 203A	0.8328
2	Al-SBA-15 103A	0.3842
3	Al-SBA-15 105A	0.5835
4	Al-SBA-15 203	0.6784
5	SBA-15 [30]	0.0400

**Figure 5.** NH₃-TPD curves for Al-SBA-15 materials

The SEM image of the Al-SBA-15 203A material shows that the aggregate shape is rod-shaped [31], while the Al-SBA-15 203 material has a hexagonal prism structure [32] (Figure 4). Based on the results obtained, there are differences in the morphology of the two Al-SBA-15 mesoporous silica materials synthesized using acidic solvents and distilled water. This difference in morphology indicates that the type of solvent affects the formation of the Al-SBA-15 structure. Research by Lee *et al.* [33] showed that the morphology of SBA-15 can be controlled through synthesis conditions.

NH₃-TPD is a method used to calculate the number of acid sites on solid catalysts [30]. Figure 5 shows a broad peak in the temperature range of 650–750°C on the NH₃-TPD curves of the four mesoporous Al-SBA-15 materials, suggesting that these materials contain acid sites with varying acid strengths. The occurrence of desorption temperature in the range above 500°C states the strong acidity of the material [14]. The acidity of each material studied can be seen in Table 4. Compared to the acidity of SBA-15 tested by Rakngam *et al.* [34], these characterization results prove that the integration of aluminium metal into the SBA-15 structure can increase the acidity of the material. The ordered acidity of the tested materials is as follows: Al-SBA-15 203A > Al-SBA-15 203 > Al-SBA-15 105A > Al-SBA-15 103A.

An increase in the mole ratio of Si to Al precursors in this study resulted in a decrease in the acidity of the synthesized material. A similar trend was reported for Al-SBA-15 synthesized without sonication at Si/Al ratios of

10 and 20 [19]. This reduction in acidity may be attributed to the decreased regularity and stability of Brønsted acid sites. At higher aluminum content, the acid sites tend to be less uniformly distributed, which may reduce the overall number of effective acid sites. Although the formation of additional Lewis acid sites occurs, these are generally weaker than Brønsted acid sites and therefore contribute less to the material's total acidity. Conversely, increasing the sonication time enhances the acidity, likely by promoting a more uniform distribution of Al and Si atoms, which facilitates the formation of additional surface acid sites [14].

4. Conclusion

The Al-SBA-15 synthesized in this study exhibits mesoporous silica characteristics, with a surface area of 718–785 m²/g, pore diameter of 4.81–5.96 nm, and pore volume of 0.92–1.07 cm³/g. Optimization of the synthesis conditions, particularly the use of distilled water as solvent and the application of optimal sonication time, proved effective in increasing the surface area. FTIR spectra confirmed the presence of siloxane, silanol, and hydroxyl functional groups, while SAXRD patterns showed a two-dimensional hexagonal structure (p6mm) with indications of changes in lattice spacing due to the mole ratio of Si and Al precursors and the type of solvent used. The morphological variations identified through SEM analysis, namely hexagonal prisms in Al-SBA-15 203 and rod shapes in Al-SBA-15 203A, indicate that the solvent plays an important role in directing the growth of mesoporous structures. In addition, NH₃-TPD analysis showed that the acidity of the materials varied between 0.38 and 0.83 mmol/g, with Al-SBA-15 203A achieving the highest acidity, indicating the potential of these materials for high acidity-based catalytic applications. Overall, these results confirm the importance of synthesis parameter control in designing Al-SBA-15 materials with optimized texture, structure, and acidity properties.

Acknowledgement

The authors would like to thank the Ministry of Research, Technology, and Higher Education of the Republic of Indonesia for financial assistance in this research through the World Research Grant with contract number 031/E5/PG/02.00.PL/2023.

References

- [1] Dieter Lenoir, Karl-Werner Schramm, Joseph O. Lalah, Green Chemistry: Some important forerunners and current issues, *Sustainable Chemistry and Pharmacy*, 18, (2020), 100313 <https://doi.org/10.1016/j.scp.2020.100313>
- [2] Patrick Schmidt-Winkel, Wayne W. Lukens, Peidong Yang, David I. Margolese, John S. Lettow, Jackie Y. Ying, Galen D. Stucky, Microemulsion Templating of Siliceous Mesoporous Cellular Foams with Well-Defined Ultralarge Mesopores, *Chemistry of Materials*, 12, 3, (2000), 686–696 <https://doi.org/10.1021/cm991097v>
- [3] Eckart Krämer, Stephan Förster, Christine Göltner, Markus Antonietti, Synthesis of nanoporous silica with new pore morphologies by templating the assemblies of ionic block copolymers, *Langmuir*, 14,

- 8, (1998), 2027–2031 <https://doi.org/10.1021/la9712505>
- [4] T. Sen, G. J. T. Tiddy, J. L. Casci, M. W. Anderson, Macro-cellular silica foams: synthesis during the natural creaming process of an oil-in-water emulsion, *Chemical Communications*, 17, (2003), 2182–2183 <https://doi.org/10.1039/B303349J>
- [5] Dirgarini J. N. Subagyo, Zhijian Liang, Gregory P. Knowles, Alan L. Chaffee, Amine modified mesoporous siliceous foam (MCF) as a sorbent for CO₂, *Chemical Engineering Research and Design*, 89, 9, (2011), 1647–1657 <https://doi.org/10.1016/j.cherd.2011.02.019>
- [6] L. Calvillo, V. Celorrio, R. Moliner, P. L. Cabot, I. Esparbé, M. J. Lázaro, Control of textural properties of ordered mesoporous materials, *Microporous and Mesoporous Materials*, 116, 1, (2008), 292–298 <https://doi.org/10.1016/j.micromeso.2008.04.015>
- [7] Supriyo Bhattacharya, Benoit Coasne, Francisco R. Hung, Keith E. Gubbins, Modeling Triblock Surfactant Templated Mesoporous Silicas (MCF and SBA-15): A Mimetic Simulation Study, in: P.L. Llewellyn, F. Rodriguez-Reinoso, J. Rouquerol, N. Seaton (Eds.) *Studies in Surface Science and Catalysis*, Elsevier, 2007, [https://doi.org/10.1016/S0167-2991\(07\)80068-1](https://doi.org/10.1016/S0167-2991(07)80068-1)
- [8] Jaeho Lee, Younggeun Park, Pil Kim, Heesoo Kim, Jongheop Yi, Preparation of NaCl-incorporated plugged mesoporous silica using a cost-effective precursor and applications to the hydrodechlorination of chlorinated hydrocarbons, *Journal of Materials Chemistry*, 14, 6, (2004), 1050–1056 <https://doi.org/10.1039/B309991A>
- [9] R. R. Dirgarini J. N. Subagyo, Sri A. Putri, Maykel Manawan, Mamun Mollah, Rudy A. Nugroho, Rahmat Gunawan, Catalytic Pyrolysis of the Green Microalgae *Botryococcus braunii* over Ni/SBA-15 Prepared by the Ultrasonic-Assisted Sol-Gel Method, *ACS Omega*, 8, 9, (2023), 8582–8595 <https://doi.org/10.1021/acsomega.2c07748>
- [10] Norihito Hiyoshi, Katsunori Yogo, Tatsuki Yashima, Adsorption characteristics of carbon dioxide on organically functionalized SBA-15, *Microporous and Mesoporous Materials*, 84, 1, (2005), 357–365 <https://doi.org/10.1016/j.micromeso.2005.06.010>
- [11] Ming Bo Yue, Lin Bing Sun, Yi Cao, Zhu Ji Wang, Ying Wang, Qing Yu, Jian Hua Zhu, Promoting the CO₂ adsorption in the amine-containing SBA-15 by hydroxyl group, *Microporous and Mesoporous Materials*, 114, 1, (2008), 74–81 <https://doi.org/10.1016/j.micromeso.2007.12.016>
- [12] P. Van Der Voort, P. I. Ravikovitch, K. P. De Jong, M. Benjelloun, E. Van Bavel, A. H. Janssen, A. V. Neimark, B. M. Weckhuysen, E. F. Vansant, A New Templated Ordered Structure with Combined Micro- and Mesopores and Internal Silica Nanocapsules, *The Journal of Physical Chemistry B*, 106, 23, (2002), 5873–5877 <https://doi.org/10.1021/jp025642i>
- [13] Lin Zhu, Hongxia Qu, Lei Zhang, Qiangfei Zhou, Direct synthesis, characterization and catalytic performance of Al-Fe-SBA-15 materials in selective catalytic reduction of NO with NH₃, *Catalysis Communications*, 73, (2016), 118–122 <https://doi.org/10.1016/j.catcom.2015.10.023>

- [14] R. R. Dirgarini Julia Nurlianti Subagyono, Nabila Mutiara Madani, Chintya Zalza Laola Claudia Buyu Prechisilia, Nabilah Sinar Sahirah, Devira Ulva Utami, Assyfa Machmudah Qosim, Mohd Asyraf Kassim, Rahmat Gunawan, Veliyana Londong Allo, Pyrolysis of microalgae over Ni/Al-SBA-15 and Ni/Ga-SBA-15 catalysts prepared using a low-acidity solvent and ultrasonic-assisted sol-gel method, *Journal of Analytical and Applied Pyrolysis*, 186, (2025), 106935 <https://doi.org/10.1016/j.jaap.2024.106935>
- [15] Dongyuan Zhao, Qisheng Huo, Jianglin Feng, Bradley F. Chmelka, Galen D. Stucky, Nonionic Triblock and Star Diblock Copolymer and Oligomeric Surfactant Syntheses of Highly Ordered, Hydrothermally Stable, Mesoporous Silica Structures, *Journal of the American Chemical Society*, 120, 24, (1998), 6024–6036 <https://doi.org/10.1021/ja974025i>
- [16] Siti Sarah, R. R. Dirgarini Julia Nurlianti Subagyono, Veliyana Londong Allo, Rahmat Gunawan, Synthesis and characterization of mesoporous silica SBA-15 prepared by the ultrasonic assisted-sol gel method, *AIP Conference Proceedings*, 3095, 1, (2024), 030003 <https://doi.org/10.1063/5.0204746>
- [17] Hongfei Liu, Shengfu Ji, Hao Yang, Huan Zhang, Mi Tang, Ultrasonic-assisted ultra-rapid synthesis of monodisperse meso-SiO₂@Fe₃O₄ microspheres with enhanced mesoporous structure, *Ultrasonics Sonochemistry*, 21, 2, (2014), 505–512 <https://doi.org/10.1016/j.ultsonch.2013.08.010>
- [18] Ahmed El-Fiqi, Mohamed Bakry, Facile and rapid ultrasound-mediated synthesis of spherical mesoporous silica submicron particles with high surface area and worm-like mesoporosity, *Materials Letters*, 281, (2020), 128620 <https://doi.org/10.1016/j.matlet.2020.128620>
- [19] R. R. Dirgarini J. N. Subagyono, Marc Marshall, W. Roy Jackson, Anthony R. Auxilio, Yi Fei, Alan L. Chaffee, Upgrading Microalgal Biocrude Using NiMo/Al-SBA-15 as a Catalyst, *Energy & Fuels*, 34, 4, (2020), 4618–4631 <https://doi.org/10.1021/acs.energyfuels.9b04171>
- [20] Francisco Gustavo Hayala Silveira Pinto, Vinícius Patrício da Silva Caldeira, Jhonny Villarreal-Rocha, Karim Sapag, Sibebe Berenice Castellã Pergher, Anne Gabriella Dias Santos, Al/SBA-15 Mesoporous Material: A Study of pH Influence over Aluminum Insertion into the Framework, *Nanomaterials*, 14, 2, (2024), 208 <https://doi.org/10.3390/nano14020208>
- [21] Obaid F. Aldosari, Mosaed S. Alhumaimess, Mohamed A. Betiha, Emad A. Ahmed, Laila M. Alhaidari, Afnan Altwala, Hassan M. A. Hassan, Characterization and Catalytic Performance of Al-SBA-15 Catalyst Fabricated Using Ionic Liquids with High Aluminum Content, *Catalysts*, 13, 11, (2023), 1395 <https://doi.org/10.3390/catal13111395>
- [22] Wenlei Xie, Libing Hu, Biguanide-functionalized mesoporous SBA-15 silica as an efficient solid catalyst for interesterification of vegetable oils, *Food Chemistry*, 197, (2016), 92–99 <https://doi.org/10.1016/j.foodchem.2015.10.103>
- [23] Lin-Bing Sun, Xiao-Qin Liu, Hong-Cai Zhou, Design and fabrication of mesoporous heterogeneous basic catalysts, *Chemical Society Reviews*, 44, 15, (2015), 5092–5147 <https://doi.org/10.1039/C5CS00090D>
- [24] Matthias Thommes, Katsumi Kaneko, Alexander V. Neimark, James P. Olivier, Francisco Rodriguez-Reinoso, Jean Rouquerol, Kenneth S.W. Sing, Physisorption of gases, with special reference to the evaluation of surface area and pore size distribution (IUPAC Technical Report), *Pure and Applied Chemistry*, 87, 9–10, (2015), 1051–1069 <https://doi.org/10.1515/pac-2014-1117>
- [25] Anton S. Shalygin, Ivan V. Kozhevnikov, Evgeny Yu Gerasimov, Andrey S. Andreev, Olga B. Lapina, Oleg N. Martyanov, The impact of Si/Al ratio on properties of aluminosilicate aerogels, *Microporous and Mesoporous Materials*, 251, (2017), 105–113 <https://doi.org/10.1016/j.micromeso.2017.05.053>
- [26] Kenneth S. Suslick, Sonochemistry, *Science*, 247, 4949, (1990), 1439–1445 <https://doi.org/10.1126/science.247.4949.1439>
- [27] Aharon Gedanken, Using sonochemistry for the fabrication of nanomaterials, *Ultrasonics Sonochemistry*, 11, 2, (2004), 47–55 <https://doi.org/10.1016/j.ultsonch.2004.01.037>
- [28] Timothy J. Mason, John P. Lorimer, Synthesis, in: *Applied Sonochemistry: Uses of Power Ultrasound in Chemistry and Processing*, 2002, <https://doi.org/10.1002/352760054X.ch3>
- [29] Tianwen Wang, Yuanzhi Li, Jichun Wu, Yaqi Hu, Pivotal role of pH value in the preparation of mesoporous silica with high surface area for toluene adsorption, *Materials Letters*, 364, (2024), 136381 <https://doi.org/10.1016/j.matlet.2024.136381>
- [30] Felix Hemmann, Christian Jaeger, Erhard Kemnitz, Comparison of acidic site quantification methods for a series of nanoscopic aluminum hydroxide fluorides, *RSC Advances*, 4, 100, (2014), 56900–56909 <https://doi.org/10.1039/C4RA09477H>
- [31] M. Gómez-Cazalilla, J. M. Mérida-Robles, A. Gurbani, E. Rodríguez-Castellón, A. Jiménez-López, Characterization and acidic properties of Al-SBA-15 materials prepared by post-synthesis alumination of a low-cost ordered mesoporous silica, *Journal of Solid State Chemistry*, 180, 3, (2007), 1130–1140 <https://doi.org/10.1016/j.jssc.2006.12.038>
- [32] Daowei Gao, Aijun Duan, Xin Zhang, Zhen Zhao, Hong E, Jianmei Li, Hai Wang, Synthesis of NiMo catalysts supported on mesoporous Al-SBA-15 with different morphologies and their catalytic performance of DBT HDS, *Applied Catalysis B: Environmental*, 165, (2015), 269–284 <https://doi.org/10.1016/j.apcatb.2014.10.034>
- [33] Hyung Ik Lee, Jin Hoe Kim, Galen D. Stucky, Yifeng Shi, Chanh Pak, Ji Man Kim, Morphology-selective synthesis of mesoporous SBA-15 particles over micrometer, submicrometer and nanometer scales, *Journal of Materials Chemistry*, 20, 39, (2010), 8483–8487 <https://doi.org/10.1039/COJMO0820F>
- [34] Issaraporn Rakngam, Nattawut Osakoo, Jatuporn Wittayakun, Narong Chanlek, Aniwat Pengsawang, Narongrit Sosa, Teera Butburee, Kajornsak Faungnawakij, Pongtanawat Khemthong, Properties of mesoporous Al-SBA-15 from one-pot hydrothermal synthesis with different aluminum precursors and catalytic performances in xylose conversion to furfural, *Microporous and Mesoporous Materials*, 317, (2021), 110999 <https://doi.org/10.1016/j.micromeso.2021.110999>